

A Novel Method for Implementation of Frameless StereoEEG in Epilepsy Surgery

Mark Nowell, MA, MRCS*‡§

Roman Rodionov, PhD*‡

Beate Diehl, MD, PhD*‡

Tim Wehner, MD, PhD*‡

Gergely Zombori, PhD¶

Jane Kinghorn, PhD*

Sebastien Ourselin, PhD¶

John Duncan, FRCP,

FMedSci*‡

Anna Miserocchi, MD*§

Andrew McEvoy, FRCS*§

*Department of Clinical and Experimental Epilepsy, UCL Institute of Neurology, London, United Kingdom; ‡Epilepsy Society, MRI Unit, Chalfont St. Peter, United Kingdom; §Department of Neurosurgery, National Hospital for Neurology and Neurosurgery, London, United Kingdom; ¶Centre of Medical Imaging and Computing, UCL, London, United Kingdom

Correspondence:

Mark Nowell, MA, MRCS,
Box 29, National Hospital for
Neurology and Neurosurgery,
Queen Square,
London, UK,
WC1N 3BG.
E-mail: m.nowell@ucl.ac.uk

Received, April 22, 2014.

Accepted, August 15, 2014.

Published Online, August 25, 2014.

Copyright © 2014 by the Congress of Neurological Surgeons. This is an open access article distributed under the Creative Commons Attribution License, which permits unrestricted use, distribution, and reproduction in any medium, provided the original work is properly cited.

BACKGROUND: Stereoelectroencephalography (SEEG) is an invasive diagnostic procedure in epilepsy surgery that is usually implemented with frame-based methods.

OBJECTIVE: To describe a new technique of frameless SEEG and report a prospective case series at a single center.

METHODS: Image integration and planning of electrode trajectories were performed preoperatively on specialized software and exported to a Medtronic S7 StealthStation. Trajectories were implemented by frameless stereotaxy using percutaneous drilling and bolt insertion.

RESULTS: Twenty-two patients went this technique, with the insertion of 187 intracerebral electrodes. Of 187 electrodes, 175 accurately reached their neurophysiological target, as measured by postoperative computed tomography reconstruction and multimodal image integration with preoperative magnetic resonance imaging. Four electrodes failed to hit their target due to extradural deflection, and 3 were subsequently resited satisfactorily. Eight electrodes were off target by a mean of 3.6 mm (range, 0.9-6.8 mm) due to a combination of errors in bolt trajectory implementation and bending of the electrode. There was 1 postoperative hemorrhage that was clinically asymptomatic and no postoperative infections. Sixteen patients were offered definitive cortical resections, and 6 patients were excluded from resective surgery.

CONCLUSION: Frameless SEEG is a novel and safe method for implementing SEEG and is easily translated into clinical practice.

KEY WORDS: Epilepsy, Frameless stereotaxy, StereoEEG

Operative Neurosurgery 10:525–534, 2014

DOI: 10.1227/NEU.0000000000000544

Stereoelectroencephalography (SEEG) is a diagnostic procedure in epilepsy surgery, in which multiple intracranial depth electrodes are placed to record electrical activity in selected cortical and subcortical structures. SEEG is performed in patients with medically refractory focal epilepsy who are considered to have a reasonable chance of progressing to potentially curative surgery, but in whom noninvasive presurgical evaluation has not sufficiently localized the epileptogenic zone. There are several advantages with SEEG over subdural grid electrode implantations, including the capture of seizure activity in 3 dimensions, better coverage in deep cortical and subcortical areas, and the avoidance of a craniotomy and the associated risks of infection. The major disadvantage of SEEG

is that there is less spatial resolution for mapping eloquent functions on the cortical surface. This can be overcome, however, if a suitable number of depth electrodes are placed, and the findings of functional imaging are also considered.

SEEG implementation is a well-established frame-based technique with the precision required to implement avascular electrode trajectories and reach targets that are identified by analysis of noninvasive data. The technique was first described by Talairach and Bancaud, who used stereoscopic teleangiography in frame-based stereotactic conditions.^{1,2} In modern practice, the workflow has been simplified by several groups. In Milan, a 1-step technique is described that uses 3-dimensional (3-D) digital subtraction angiography with a mobile cone-beam computed tomography (CT) scanner in frameless conditions in preference to stereotactic teleangiography. The implantation is implemented later in a Talairach

ABBREVIATIONS: EA, accuracy of electrode delivery; SEEG, stereoelectroencephalography

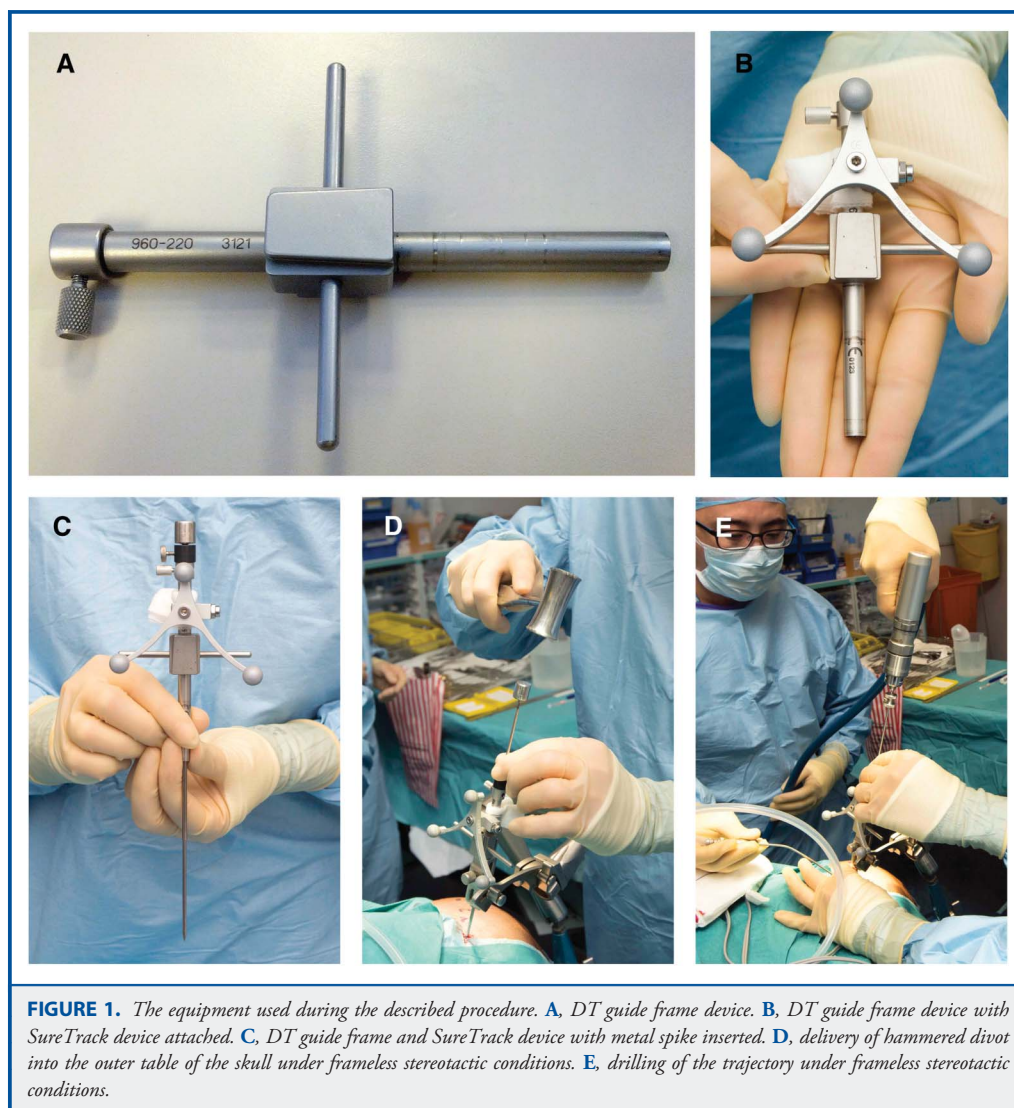
TABLE 1. Specifications of the Basic Imaging Package Used in the Implementation of Frameless Stereoelectroencephalography^a

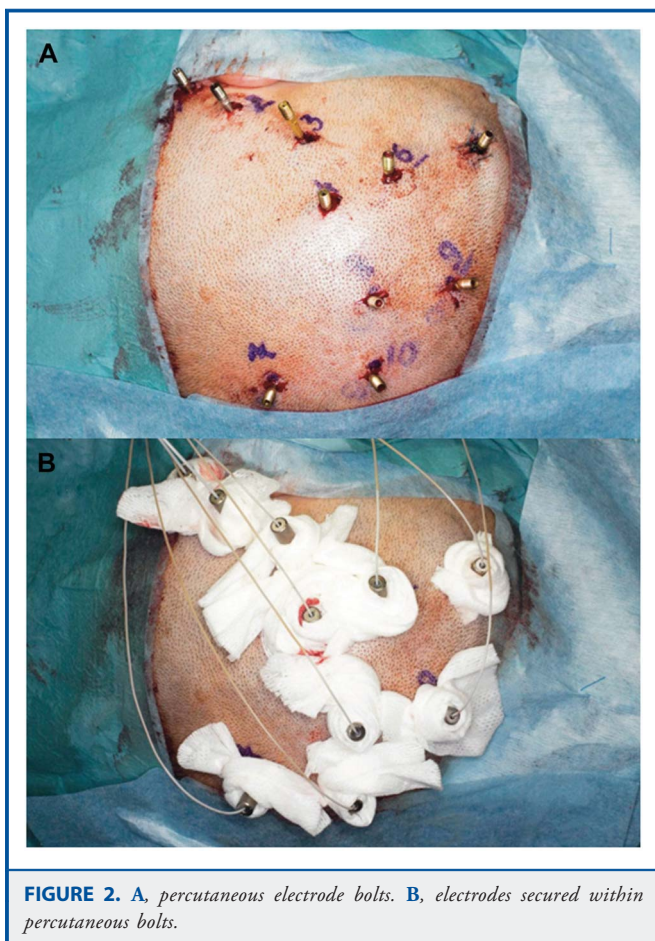
Imaging Modality	Scanner	Structure Shown	Slice Thickness (mm)	Voxel Size (mm)	Resolution
Navigation T1 with gadolinium MRI	Siemens Avanto 1.5	Brain	1.5	0.488 × 0.488 × 1.5	512 × 512 × 144
3D phase contrast MRI	Siemens Avanto 1.5	Veins	1	0.86 × 0.86 × 1.0	256 × 256 × 160
CT angiogram	Somatom Definition AS	Arteries	0.75	0.43 × 0.43 × 0.75	512 × 512 × 383

^aMRI, magnetic resonance imaging; 3D, 3-dimensional; CT, computed tomography.

stereotactic frame.³ In Cleveland, on-table 3-D CT angiography is performed in a Leksell frame before frame-based implementation.⁴ There is also experience using the stereotactic robotic Neuromate (RENISHAW, Gloucestershire, United Kingdom) in the frame-based placement of depth electrodes.⁵

The advantage of frame-based techniques is the accuracy of electrode delivery to a predefined target, with a quoted median target point localization error of 2.02 mm, an interquartile range of 1.37 to 2.96 mm, and major complication rate of 2.4%.³ However, there are several disadvantages that include potential





patient discomfort, additional time for frame placement, restricted access to the surgical field, and a limited ability to define new trajectories in real time during surgery. Additionally, there are the costs associated with specialist equipment, the need

for additional intraoperative imaging and training in frame-based techniques.

We describe our technique and experience in the implementation of frameless SEEG at a single center.

METHODS

Preparation

Patients underwent routine presurgical evaluation for epilepsy surgery at the National Hospital for Neurology and Neurosurgery, and individuals needing SEEG were selected on a case-by-case basis after a multidisciplinary team meeting and subsequent focused strategy meeting led by neurophysiologists. These patients underwent preoperative navigation T1-weighted volumetric magnetic resonance imaging (MRI) with gadolinium enhancement, 3-D phase contrast MRI for visualization of veins, and CT angiography for visualization of arteries. For a detailed description of imaging specifications, see Table 1.

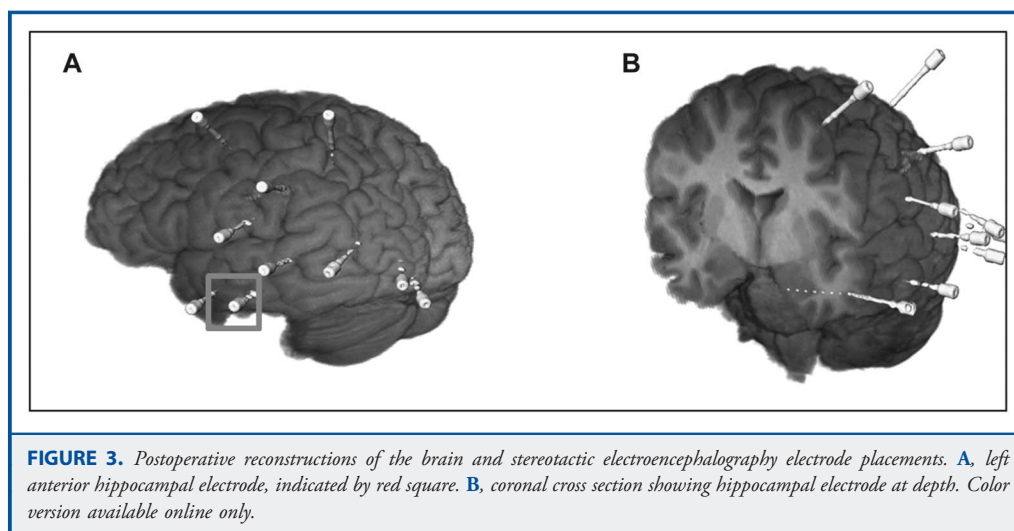
Image integration was performed with the EpiNav software system (Centre of Medical Imaging and Computing, University College London, United Kingdom), and any relevant additional functional and structural imaging performed during evaluation was incorporated.⁶

Preoperative surgical planning of electrode implantations with 3-D multimodal integration was performed by the epilepsy surgery team, including 2 neurosurgeons on the EpiNav software system (Centre of Medical Imaging and Computing). The planned arrangement was then exported to an S7 StealthStation (Medtronic, Minneapolis, Minnesota) in the operating theater. Each planned trajectory was checked by 2 neurosurgeons on the StealthStation before implementation.

Surgery

Patients underwent a fiducial marker registration.⁷ The crucial steps of SEEG implementation comprised the following:

- Apply the SureTrack tool to Guide Frame DT and register to S7 StealthStation
- Select a planned trajectory on the StealthStation
- Mark the entry point on the scalp for electrode entry and perform a stab incision



- Line up manually the Guide Frame DT, loaded on the Medtronic arm, using the Guidance View option
- Lock trajectory, and use a system of custom-designed reducing tubes to perform the following steps through the Guide Frame DT with real-time neuronavigational feedback:
 - Create a hammered divot in the outer table of the skull using a custom-designed spike (Ad-Tech Medical Instrument Corporation, Racine, Wisconsin)
 - Drill through the skull and perforate the dura
 - Screw in electrode bolts (Ad-Tech Medical Instrument Corporation) (outer diameter, 1.9-2.5 mm; length, 21 mm)
- Using the Stealth Probe, reset the entry point of the planned trajectory to the tip of the electrode bolt to calculate the updated length of electrode
- Use a rigid extraventricular drain stylet (8F Silverline; Spiegelberg, Hamburg, Germany) to ensure dural opening and create the intraparenchymal trajectory for the electrode, minimizing subsequent electrode deviation. The stylet is set to correct intracranial length using plastic stopper
- Insert electrode to appropriate length and secure with screw top, Spencer depth electrodes (range from 4, 6, 8, and 10 contacts) (Ad-Tech, Medical Instrument Corporation) (Figures 1 and 2).

A postoperative CT head scan is performed 4 hours after surgery to check the placement of the electrodes and exclude an intracranial hemorrhage. The patient is then transferred to the telemetry ward for intracranial electroencephalographic recording.

Accuracy

Accuracy of electrode placement is assessed in 2 ways:

Qualitative Assessment

The postoperative CT is coregistered with the presurgical 3-D multimodal models using AMIRA software (FEI Visualization Sciences Group, Burlington, MA), and the individual electrodes are segmented as 3-D models. The position of the electrodes relative to the cortical and subcortical structures is examined by the neurophysiologist in association with the neurophysiological findings. A dichotomous assessment is made of whether the electrodes are reaching their designated targets (See Figure 3).

Quantitative Assessment

The postoperative CT scan is uploaded onto the S7 StealthStation, and coregistered with the patient's preoperative imaging using the StealthMerge tool as part of the Stealth7 software. The electrodes are segmented out as 3-D models, and for each electrode model, a new implemented trajectory is created, passing directly through the bolt trajectory. A quantitative comparison is then performed between the planned trajectory, implemented trajectory, and actual electrode placement (Figures 4 and 5). This gives measurements of the accuracy of trajectory delivery, the degree of intraparenchymal electrode deviation, and a final assessment of the accuracy of electrode delivery (EA), which corresponds to the lateral perpendicular shift at the planned target point.

RESULTS

Demographics

Twenty-two patients were included in this case series. The demographics are shown in Table 2. There were 9 nonlesional cases and 13 lesional cases. There were 7 temporal cases with 2

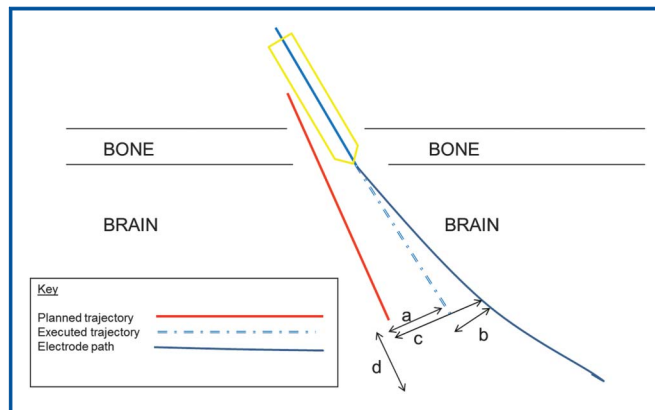


FIGURE 4. Schematic representation of quantitative measures used. *a*, trajectory accuracy: lateral shift between planned and executed trajectories, in plane perpendicular to executed trajectory that passes through target point. *b*, electrode deviation: lateral shift between electrode contact and executed trajectory, in plane perpendicular to executed trajectory that passes through target point. *c*, electrode accuracy: lateral shift between electrode contact and planned trajectory, in plane perpendicular to planned trajectory at target point. *d*, deviation of electrode length from planned trajectory, as seen in trajectory view on S7 StealthStation.

bitemporal cases, and there were 13 extratemporal cases. The median time for implantation was 137 minutes (range, 80-167 minutes).

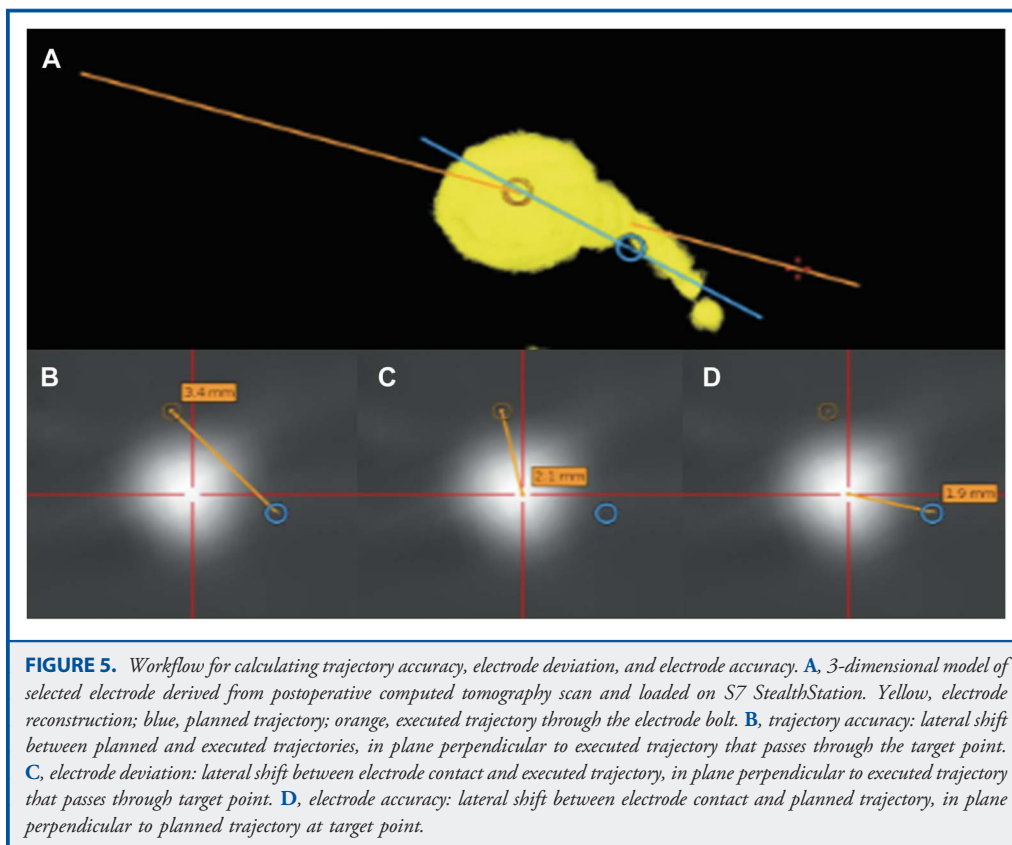
Assessment of Implantation Accuracy

Figure 6 demonstrates the segmentation of electrodes for patient 8, derived from postoperative CT, reconstructed on the 3-D models, and overlaid on the planned trajectories on the S7 StealthStation. Figures 7 and 8 show the implantation in patient 19; the typical approach to implanting the mesial temporal structures is demonstrated, perpendicular to the long axis of the hippocampus with entry points in the middle temporal gyrus. The overall qualitative and quantitative assessments are shown in Tables 3 and 4.

There were 187 electrodes inserted in total, with 175 electrodes deemed to have reached their planned neurophysiological target. The mean electrode accuracy was 3.66 mm, with a standard deviation of 2.21 mm, a median of 3.45 mm, and an interquartile range of 3.6 mm.

There was no significant difference between the accuracy of implantation of mesial temporal vs extratemporal electrodes. A quantitative comparison of EA values showed a tendency to improved EA values for mesial temporal electrodes, although this was not statistically significant ($P = .057$, 2-tailed paired t test type 2). A qualitative comparison of target hitting showed no difference between mesial temporal and extratemporal electrodes ($P = .33$, Fisher exact test).

Twelve electrodes were deemed to have missed their neurophysiological targets in patients 1, 3, 5, 6, 8, 12, 13, and 18. Four of these electrodes were subject to significant extradural deflection, and 3 of these were satisfactorily resited at a later date with accurate targeting. The extradural deflection occurred early on in our



experience, before the use of a rigid stylet to ensure dural breach and to create an intraparenchymal track. Table 5 summarizes the details of all the missed electrodes. Figures 9 and 10 show examples of postoperative reconstructions of implanted electrodes deemed to have missed their targets.

Outcomes

Sixteen patients were offered cortical resections on the basis of recordings from the SEEG implantation. Six patients were excluded from definitive resective surgery based on the SEEG recordings. There was 1 hemorrhagic complication in patient 18, evident on postoperative CT. The blood was in the sylvian cistern on the side of the implantation, with no obvious cause of bleeding. The patient was asymptomatic with no neurological deficits, and no further treatment was required. There were no cases of infection. All electrodes were removed after recording with no complications. One patient reported chest pain after, requiring inpatient assessment to exclude a pulmonary embolus and cardiac event. No underlying cause was found for the chest pain, and the patient made a full recovery.

DISCUSSION

Burr hole biopsy of intracerebral tumors is routinely done using frameless stereotaxy in preference to frame-based methods,

although it is generally accepted that frameless techniques confer lower degrees of accuracy of registration.⁸ This technique confers a level of precision that is considered acceptable for the majority of cases. Of course, there remain indications for frame-based biopsy, such as deep-seated small tumors, when the added precision is necessary.

This situation is analogous to SEEG in which multiple electrodes are placed into relatively broad targets. The twin concerns with SEEG are accurate targeting and avoidance of cortical blood vessels. We believe that in selected cases, electrode arrangements can be designed with the necessary safety profile for implementation with a frameless technique.

Mehta et al⁹ described the frameless delivery of depth electrodes through burr holes and craniotomy sites by using a slotted, custom-designed adaptor built to interface with a commercially available neuronavigation system (StealthStation Guide Frame-DT and 960-525 StealthFighter). The need for burr holes has several disadvantages, limiting the number of electrodes that can be placed at any one time and limiting the subsequent design of any bone flap in the future. Also, larger openings generally predispose to increased risks of postoperative infection.

Shamir et al¹⁰ assessed the accuracy of delivery of the Ommaya ventricular catheter using the Medtronic neuronavigation system

TABLE 2. Demographics of the Patient Group Undergoing Frameless Stereoelectroencephalography in This Case Series^a

Patient	Age, y/Sex	Years Since Diagnosis	Lesional	Description	Presumed EZ
1	41/M	16	Yes	Gray matter heterotopia/HS	Right temporal
2	24/F	23	Equivocal	Focal cortical dysplasia	Left parietal
3	52/M	19	Yes	HS	Left frontotemporal
4	22/M	21	No	NA	Left posterior quadrant
5	40/M	34	No	NA	Left temporocentroparietal
6	41/M	31	Yes	Encephalomalacia	Left frontocentral
7	55/F	20	No	NA	Bitemporal
8	29/M	11	Yes	Encephalomalacia	Left frontocentral
9	18/M	7	Equivocal	Focal cortical dysplasia	Right temporal
10	19/F	10	Yes	Low-grade glioma	Right occipital
11	27/M	17	No	NA	Right parieto-occipital
12	40/M	35	No	NA	Right occipital
13	22/M	11	Yes	Encephalomalacia	Left posterior quadrant
14	32/M	15	Yes	Low-grade tumor	Right temporal
15	37/F	17	Yes	Low-grade tumor	Right posterior quadrant
16	19/M	14	No	NA	Right frontal
17	44/M	38	No	NA	Right frontocentral
18	34/F	29	Yes	Frontal atrophy	Left temporal
19	29/F	7	Yes	Focal cortical dysplasia	Bitemporal
20	42/F	16	No	NA	Right frontocentral
21	22/F	16	No	NA	Right temporal
22	29/M	21	Yes	Schizencephaly	Right temporal

^aM, male; EZ, epileptogenic zone; HS, hippocampal sclerosis; F, female; NA, not applicable.

in 15 consecutive cases, comparing the implemented plan with the planned trajectory. They found a mean target point localization error of 5.9 ± 4.3 mm and a mean shift of 3.9 ± 4.7 mm.

The technique in our case series relies on custom-designed reducing tubes and a hammered divot in the cranial outer table to

stabilize the drilled trajectory. With this technique, frameless SEEG delivered 175 of 185 electrodes to their expected target, with a mean electrode accuracy of 3.66 mm. There was improvement in implementation with experience; in the first half

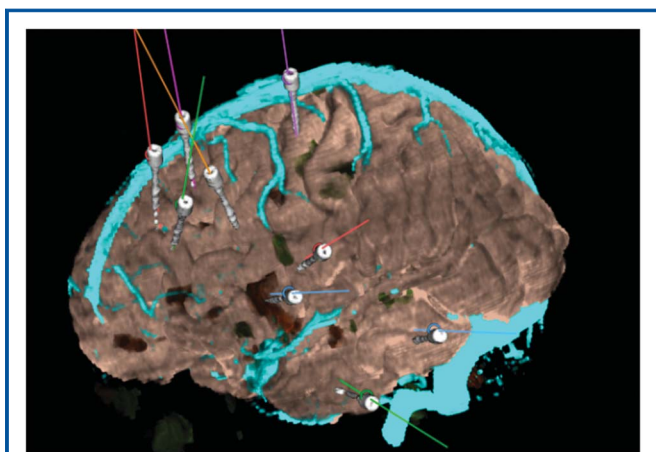


FIGURE 6. Postoperative reconstruction of electrode implantation coregistered to the preoperative 3-dimensional multimodal models and displayed on the StealthStation for patient 8.

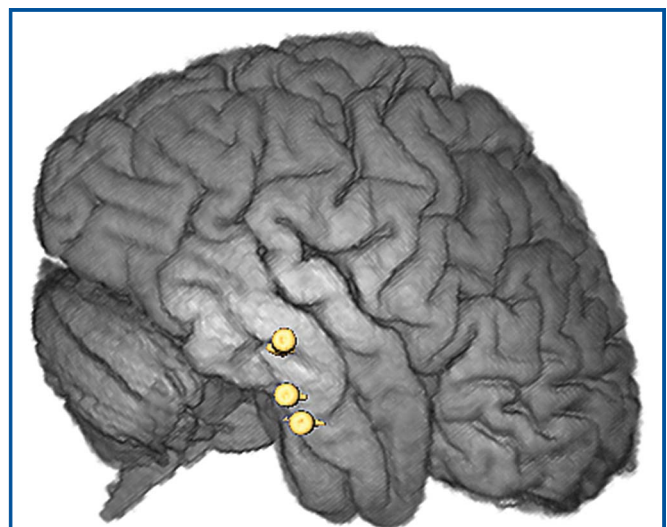


FIGURE 7. Postoperative reconstruction of electrode implantation on AMIRA software for patient 19 showing bitemporal implantation of the amygdala and hippocampus (right lateral view).

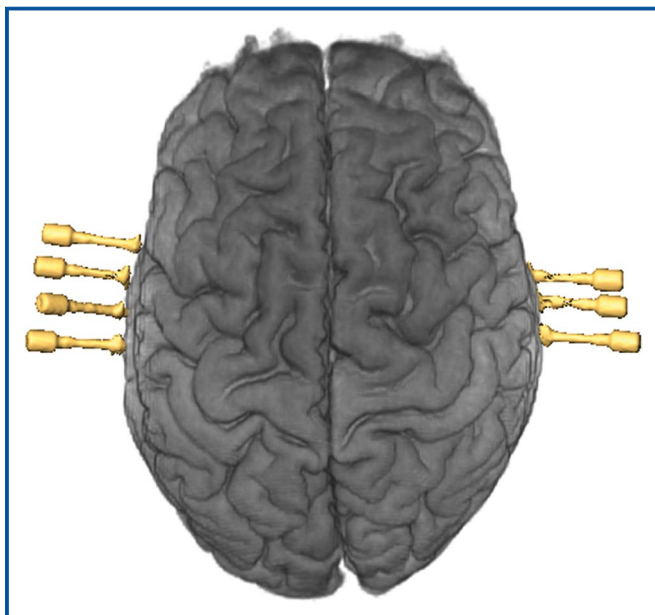


FIGURE 8. Postoperative reconstruction of electrode implantation on AMIRA software for patient 19 showing bitemporal implantation of the amygdala and hippocampus (superior view).

of the series (11 patients), 9 electrodes missed their neurophysiological target, whereas in the second half of the series, only 3 electrodes missed their target. Most importantly, there were no serious hemorrhagic complications, although we deliberately avoided trajectories that require finer accuracy, such as the transylvian route to the insula. Finally, this technique confers a level of flexibility where it is straightforward to augment an implantation with additional electrodes if further contacts are required. This was performed in patient 14 with no complications, and the additional information proved valuable to the case.

There was no significant difference between the accuracy of electrode insertion between mesial temporal and nonmesial temporal electrodes. There was, however, a tendency toward more accurate quantitative implantations in the amygdala and hippocampus. This may be due to these electrodes being very commonly placed and being placed perpendicular to the skull. Qualitatively, however, 5 of the 12 missed targets were in the mesial temporal structures. This is most likely due to the fact that these targeted structures are well defined and smaller than other more extensive extratemporal targets.

The greatest source of inaccuracy is the registration in frameless stereotaxy. The registration error associated with frameless stereotaxy is well documented and does not necessarily correlate with the registration error generated by the system.^{10,11} In our series, we used scalp fiducial marker registration and made a great effort to achieve the best registration possible. We anticipate that the use of bone fiducials should further increase the accuracy of the registration and the procedure in total, although this would also increase the presurgical invasiveness of the procedure.

TABLE 3. Outcomes of the Qualitative and Quantitative Assessments of Electrode Implantation Accuracy^a

Patient	No. of Electrodes	Qualitative Accurate Targeting	Mean Quantitative Assessment, mm			
			TA	ED	EA	L
1	5	3	6.58	0.00	6.58	2.10
2	9	9	4.50	3.43	4.80	11.46
3	8	5	2.74	2.71	3.14	4.80
4	9	9	4.02	2.82	3.56	3.16
5	7	6	4.87	1.52	5.05	4.03
6	7	5	7.01	1.80	6.20	2.02
7	7	7	6.69	3.21	5.34	4.07
8	9	8	3.14	0.73	3.08	3.51
9	10	10	4.24	1.59	3.90	0.71
10	9	9	5.12	1.97	4.87	2.83
11	10	10	4.63	1.50	4.31	3.08
12	10	9	4.50	1.14	4.24	3.02
13	10	9	6.14	2.26	5.26	3.22
14	7	7	3.64	1.66	2.94	3.66
15	7	7	3.07	1.41	2.59	1.20
16	7	7	3.94	1.33	3.57	3.17
17	7	7	2.30	0.84	2.54	2.59
18	11	10	1.85	1.15	2.05	1.95
19	7	7	2.26	1.13	3.23	1.28
20	10	10	1.34	1.19	1.57	1.62
21	8	8	0.96	1.00	1.25	1.55
22	13	13	2.74	1.74	3.25	1.76

^aTA, trajectory accuracy; ED, electrode deviation; EA, electrode accuracy; L, deviation of electrode length.

Further deterioration in electrode accuracy occurs with the drilling of the trajectory and intracranial electrode deviation. Drill trajectory was stabilized by a hammered divot in the outer table and a system of reducing tubes to deliver the drill and the bolt in a stereotactic manner. The design of the electrode trajectories was

TABLE 4. Mean Electrode Accuracy by Electrode Target

Electrode Target	No.	Mean Electrode Accuracy, mm	Missed
Amygdala	16	2.76	3
Anterior hippocampus	19	3.62	1
Posterior hippocampus	19	3.31	1
Cingulate gyrus	13	4.28	0
Orbitofrontal	16	4.47	0
Insula	15	2.83	4
Lateral temporal	12	4.30	0
Frontal	22	3.38	2
Perirolandic	14	3.99	0
Parietal	27	3.85	1
Occipital	14	3.89	0

TABLE 5. Details of the Electrodes Deemed to Have Missed Their Neurophysiological Targets^a

Patient	Electrode	Target	Electrode Accuracy, mm	Electrode Depth, mm
1	Amygdala	Inferiorly placed in entorhinal cortex	5.4	52
1	R parietal periventricular tuber	Anteriorly placed	7.3	54
3	Amygdala	Inferiorly placed in entorhinal cortex	0.9	49
3	Anterior hippocampus	Inferiorly placed	2.0	54
3	SFG to anterior insula	Extradural deflection: satisfactorily resited	1.8	47
5	Posterior insula	Extradural deflection: unsatisfactorily resited	4.3	58
6	MFG to superior lesion	Extradural deflection: satisfactorily resited	2.5	25
6	SFG to lateral lesion	Extradural deflection: satisfactorily resited	3.6	18
8	Amygdala	Inferiorly placed in entorhinal cortex	6.8	36
12	Posterior insula	Short and mesial placed in internal capsule	2.4	35
13	Posterior hippocampus	Inferiorly placed	4.1	48
18	Posterior insula	Mesially placed in striatum	2.6	55

^aMFG, middle frontal gyrus; R, right; SFG, superior frontal gyrus.

also considered; as a rule, we attempted to maintain an entry angle to the outer table to within 10° of the perpendicular to minimize any slip of the drill. With regard to electrode deviation, changes were made to the technique during the series as experience was acquired. Of the 12 of /187 electrodes that missed their target, 4 electrodes deviated significantly during their intracranial course. This deviation was mainly caused by extradural deflection, and 3 electrodes were satisfactorily resited through the same bolt at a later date. In addition, some electrode deviation was observed intraparenchymally following large white matter tracts due to the nonrigid nature of the electrodes. From patient 7 onward, a rigid stylet was passed through the bolts before passing each electrode.

This prevented any further extradural deflections and reduced clinically relevant electrode deviations.

Our case series is limited by inaccuracies in the assessment of electrode placement. The qualitative assessment relies on the registration of a postoperative CT scan with a preoperative MRI scan and rendering of the electrodes in the context of the cortical segmentation. This registration is limited by the issue of brain shift, with escape of cerebrospinal fluid during electrode implantation. The neurophysiological recordings were useful in some electrodes, confirming accurate placement within a well-defined propagation network, ie, hippocampus. However, this did not apply to the extratemporal electrodes. The issue of brain shift could

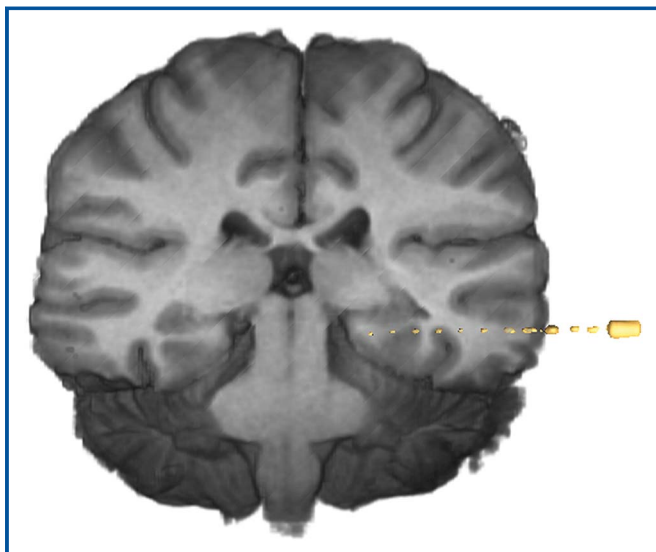


FIGURE 9. Postoperative reconstruction of electrode implantation on AMIRA software for patient 13 showing inferiorly placed hippocampal electrode (coronal view).

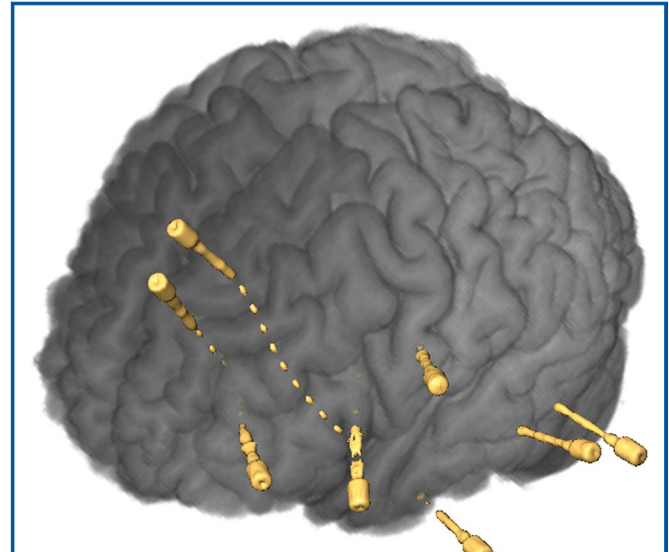


FIGURE 10. Postoperative reconstruction of electrode implantation on AMIRA software for patient 6 showing extradural deflection of electrode.

be addressed in the future by the acquisition of postoperative MRI scans, although we would not anticipate significant shift with this procedure. The necessary safety testing for the acquisition of postoperative MRI in this patient group is currently under way at our center.

The quantitative assessment used a technique first described by Shamir et al¹⁰ in the placement of ventricular access devices. The electrode accuracy is a measure of lateral shift perpendicular to and at the point of the planned trajectory target. This is not the same as the target point localization error referred to elsewhere, ie, the Euclidean distance between the planned trajectory target and the implemented electrode tip.³ The tip of the electrode is not the only point of interest in the implantation, as recordings are made from all contacts along the length of the electrodes, and our measure of electrode accuracy is sufficient to gauge electrode delivery. Unfortunately, using our software, it was not possible to extract the Euclidean distance from the electrode and planned target points.

Future work will focus on how to improve the design and implementation of SEEG. There is great interest in an automated planning system that generates electrode arrangements with improved safety profiles and greater efficiency in terms of gray matter contact. This is dependent on robust techniques to segment out critical structures such as blood vessels. There is also interest in techniques that further improve the implementation of planned electrode arrangements, including frameless robotic implantation.

CONCLUSION

Our technique of frameless SEEG is a feasible approach in selected cases. The ease of implementation makes this approach

particularly attractive for centers moving toward adoption of SEEG in the presurgical evaluation of epilepsy. However, the inferior accuracy of this method makes it less suitable for implantations of “high-risk” trajectories, which are best achieved with a conventional, frame-based technique.

A general comparison of frame-based and frameless SEEG is shown in Table 6.

Disclosure

Mark Nowell, Gergely Zombori, and Roman Rodionov are supported by a Wellcome Trust/Department of Health Programme grant (HICF 4-275, Programme Grant 97914) and are working in collaboration with Medtronic, Inc. This work was undertaken at UCLH/UCL who received a proportion of funding from the Department of Health’s NIHR UCLH Biomedical Research Centre funding scheme. John Duncan has received institutional grant support from Eisai, UCB Pharma, GlaxoSmithKline, Janssen Cilag, Medtronic, and GE Healthcare. Andrew McEvoy has received support from UCB, Baxter, and Cyberonics. The other authors have no personal, financial, or institutional interest in any of the drugs, materials, or devices described in this article.

REFERENCES

- Szikla G, Bouvier G, Hori T, Petrov V. *Angiography of the Human Brain Cortex*. Berlin, Germany: Springer; 1977.
- Talairach J, Szikla G. Application of stereotactic concepts to the surgery of epilepsy. *Acta Neurochir Suppl (Wien)*. 1980;30:35-54.
- Cardinale F, Cossu M, Castana L, et al. Stereoelectroencephalography: surgical methodology, safety and stereotactic application accuracy in 500 patients. *Neurosurgery*. 2013;72(3):353-366.
- Gonzalez-Martinez J, Mullin J, Vadera S, et al. Stereotactic placement of depth electrodes in medically intractable epilepsy. *J Neurosurg*. 2014;120(3):639-644.
- Abhinav K, Prakash S, Sandeman D. Use of robot-guided stereotactic placement of intracerebral electrodes for investigation of focal epilepsy: initial experience in the UK. *Br J Neurosurg*. 2013;27(5):704-705.
- Rodionov R, Vollmar C, Nowell M, et al. Feasibility of multimodal 3D neuroimaging to guide implantation of intracranial EEG electrodes. *Epilepsy Res*. 2013;107(1-2):91-100.
- Pfisterer W, Papadopoulos S, Drumm D, Smith K, Preul M. Fiducial versus nonfiducial neuronavigation registration assessment and considerations of accuracy. *Neurosurgery*. 2008;62(3 suppl 1):201-207.
- Price R. The advantages of frameless stereotactic biopsy over frame-based biopsy. *Br J Neurosurg*. 2003;17(1):90-91.
- Mehta A, Labar D, Dean A, et al. Frameless stereotactic placement of depth electrodes in epilepsy surgery. *J Neurosurg*. 2005;102(6):1040-1045.
- Shamir RR, Joskowicz L, Spektor S, Shoshan Y. Localization and registration accuracy in image guided neurosurgery: a clinical study. *Int J Comput Assist Radiol Surg*. 2009;4(1):45-52.
- Wang MN, Song ZJ. Classification and analysis of the errors in neuronavigation. *Neurosurgery*. 2011;68(4):1131-1143.

Acknowledgments

The authors are grateful to the Wolfson Trust and the Epilepsy Society for supporting the Epilepsy Society MRI scanner.

COMMENTS

The authors of this report present results of a single-center series of stereoelectroencephalography (SEEG) recordings with electrode insertion technique that is based on a frameless surgical approach. SEEG is an invasive diagnostic procedure in epilepsy surgery in which multiple depth electrodes are inserted to different targets to record electrical activity in the cortical and subcortical structures; traditionally, this is done using

TABLE 6. Comparison of Frame-Based and Frameless Stereoelectroencephalography^a

	Framed-Based SEEG	Frameless SEEG
Need for frame	Yes	No
Need for intraoperative imaging	Yes	No
Accuracy to target, mm	<2	>2
Stability of tool delivery	Excellent	Reasonable
Suitability for high-risk trajectories	Good	Poor
Uniformity of method	Varies among centers	Not previously described
Software	Varies among centers	Medtronic StealthStation
Restrictions to surgical field	Yes	No
Flexibility to change plans intraoperatively	Limited	Good
Ease of implementation with no specialist training	Limited	Good

^aSEEG, stereoelectroencephalography.

a well-established frame-based technique. As correctly mentioned by the authors, there are several advantages of SEEG, including the capture of seizure activity in 3 dimensions, better coverage in deep cortical and subcortical areas, and avoidance of a craniotomy and associated reduction in risk of infection. However, it is not a perfect modality, and there are obvious disadvantages related to the conventional frame-based SEEG approach, such as potential patient discomfort, additional surgical time required for frame placement, restricted access to the surgical field, and a limited ability to define new trajectory in real time during the surgery.

In this study, the authors introduced the new technique, frameless SEEG, and reported their experiences in some patients. Frameless SEEG has been shown to be a feasible approach to determine epileptogenic focus/areas in selected cases with good results and no serious complications. They also point out that the technique may easily be applied at other medical centers without the need for special equipment, which makes it more attractive to those epilepsy surgeons who do not routinely use stereotactic frames.

However, there are some issues that need to be addressed, including the inferior accuracy of this method mentioned by the authors. The suggested technical improvements in the use of frameless intraoperative navigation, such as application of a custom-designed spike for creation of divot on the bone surface and advancement of a stylet before electrode insertion may translate into improved precision of the targeting. Another concern is in the potential source of inaccuracy due to cerebrospinal fluid leak and resulting brain shift.

Because precise targeting and procedural safety are the 2 main concerns in this approach, perhaps integration of a volumetric intraoperative imaging (such as intraoperative CT or MRI) may be the way to go.

Dali Yin
Konstantin Slavin
Chicago, Illinois

The authors provide a detailed description of their technique for, and experience with, frameless stereoelectroencephalography (SEEG)—a technique used to obtain invasive EEG recordings from multiple intracranial depth electrodes for the localization of the spatial extent of an epileptic focus. As rationale for this investigation, they point out the advantages of frameless SEEG over frame-based SEEG, including better access to the surgical field, greater flexibility in placing additional electrodes intraoperatively, and shorter procedural time—although data supporting the latter point are not provided. The authors used this technique to record from 187 electrodes in 22 patients, with postoperative CT imaging verification of electrode location relative to the intended location on preoperative multimodal 3D imaging models. The authors report 1 asymptomatic hemorrhagic and no infectious complications. A mean electrode accuracy of 3.66 mm is reported, with 12 of 187 electrodes deemed to have missed the intended target. It seems likely that the threshold for this designation of a missed target would differ depending on the target structure, with different degrees of inaccuracy tolerated for different target structures, as they allude to in their discussion. The authors correctly point out that brain shift on postoperative imaging relative to preoperative studies limits the assessment of accuracy

of electrode placement and indicate that they intend to use postoperative MRI in the future to determine electrode location accuracy with greater precision.

The authors nicely describe the potential contributions to accuracy of electrode placement and furnish clear descriptions of the different measures used to assess placement, including trajectory accuracy, electrode deviation, electrode accuracy, and deviation of electrode length. The importance of hammered divots to control drill trajectory and the use of a rigid stylet to ensure dural perforation and intraparenchymal trajectory are among the steps described that they believe led to improved technical accuracy over the duration of the study. The authors note the obvious advantages and disadvantages of frameless SEEG over conventional frame-based SEEG: there may be reduction in procedure time and patient discomfort by eliminating the placement of a rigid head frame, yet accuracy is decreased relative to frame-based stereotaxy, rendering some targets unsuitable for this approach. Bone fiducials, as the authors suggest, would likely improve accuracy of the registration. Brain shift is a variable that can affect either technique, and this might suggest a role for intraoperative CT or intraoperative MRI in the future so as to visualize the target structures after the majority of the shift has occurred. Overall, the authors provide a careful description of their technique for frameless stereotactic placement of SEEG electrodes, with some valuable technical nuances described. They acknowledge that their technique is not suitable for approaches requiring submillimetric accuracy, such as the transylvian route to the insula. If more information was furnished about the depth and location of the implanted targets in this series, broader conclusions might be drawn about which targets may be more or less suitable for this technique.

Aviva Abosch
Steven Ojemann
Aurora, Colorado

Despite its extensive reported successful record, with almost 60 years of clinical use, the technical intricacy regarding the placement of SEEG depth electrodes might have contributed to its restricted clinical application in surgical centers outside Europe. In this technical report, the authors describe a novel, practical, and simplified method of frameless SEEG electrode implantation. The proposed technique is interesting because it extends the actual surgical armamentarium for the placement of depth electrodes in patients with medically intractable focal epilepsy with difficult to localize seizures. Consequently, the current technique corresponds to an alternative to the more complex and expensive methods for depth electrode placement. Although the initial clinical experience demonstrates acceptable results in terms of hemorrhagic complications, the relative low accuracy rate (in relation to other frame-based methods) may prevent its clinical application in higher vascularized cortical areas such as the perisylvian regions and insula, where a higher accuracy method is mandatory. To confirm the authors' preliminary impressions, a larger and multicenter study will be likely needed.

Jorge Gonzalez-Martinez
Cleveland, Ohio